Product energy distributions from ethylene photodissociation at 193 nm: A DFT direct classical trajectory study

ARTICLE *in* CHEMICAL PHYSICS LETTERS · FEBRUARY 2003

Impact Factor: 1.9 · DOI: 10.1016/S0009-2614(02)01894-8

4 AUTHORS, INCLUDING:

Emilio Martinez-Nuñez
University of Santiago de Compostela
86 PUBLICATIONS **1,020** CITATIONS
SEE PROFILE

Antonio Fernández-Ramos
University of Santiago de Compostela
84 PUBLICATIONS **1,833** CITATIONS
SEE PROFILE

Saulo A Vázquez
University of Santiago de Compostela
90 PUBLICATIONS **1,046** CITATIONS
SEE PROFILE

Available online at www.sciencedirect.com
SCIENCE DIRECT®
Chemical Physics Letters 369 (2003) 1–7
CHEMICAL PHYSICS LETTERS
www.elsevier.com/locate/cplett

Product energy distributions from ethylene photodissociation at 193 nm: a DFT direct classical trajectory study

Emilio Martínez-Núñez *, Antonio Fernández-Ramos, Angeles Peña-Gallego, Saulo A. Vázquez

Departamento de Química Física, Facultade de Quimica, Universidad de Santiago de Compostela, Avda. das Ciencias, s/n Santiago de Compostela E-15706, Spain

Received 27 October 2002

Abstract

The photodissociation of ethylene at 193 nm was studied by a B3LYP/6-31G(d) direct trajectory method, in which the trajectories were initialized from the two exit barriers associated to molecular hydrogen formation. The calculated translational energies and the H_2 rotational and vibrational states distributions are in good agreement with the experimental data. Our results, together with those obtained in a previous trajectory study [A. Peña-Gallego, E. Martínez-Núñez, S.A. Vázquez, Chem. Phys. Lett. 353 (2002) 418], are in line with the conclusion that the dissociation dynamics is statistical in the reactant phase space, although the product energy distributions for both channels are nonstatistical.

1. Introduction

The photodissociation of ethylene has been extensively investigated during the past decade, especially by Lee and co-workers [1–7]. The primary channels in the VUV range are associated with H_2 and H eliminations:

$$C_2H_4 \rightarrow HC{\equiv}CH + H_2 \quad (1a)$$

$$C_2H_4 \rightarrow H_2C{=}C: + H_2 \quad (1b)$$

$$C_2H_4 \rightarrow CHCH_2 + H \quad (2a)$$

$$CHCH_2 \rightarrow HC{\equiv}CH + H \quad (2b)$$

There are several experimental and theoretical indications that suggest that these reactions take place on the ground electronic state, after rapid internal conversion from the initially excited state [1,3,6,8–10].

Controversy appeared in the literature concerning the possibility of nonstatistical effects in the photodissociation of ethylene. Bersohn and coworkers [8] found very good agreement between the experimental and RRKM ratios of H atoms to D atoms released from CH_2CD_2 and *trans*-HDCCDH, and concluded that the dissociation

* Corresponding author. Fax: +34-981-595012.
E-mail address: uscqfemn@cesga.es (E. Martínez-Núñez).

0009-2614/03/$ - see front matter
PII: S0009-2614(02)01894-8

takes place from a hot internally equilibrated ground state molecule. By contrast, Lee and coworkers [1,3,5,6] found poor agreement between the experimental and RRKM H_2:HD:D_2 branching ratios in products for the deuterated species D_2CCH_2, *cis*-HDCCDH and *trans*-HDCCDH, and suggested that the dynamics is nonstatistical. More specifically, they stated that 'it seems likely the excited electronic state converts to the ground state surface crossing in either 1,2 E (reaction 1a) or 1,1 E (1b) channel, or both, resulting in nonstatistical dynamics that cannot be described by the RRKM theory' [5]. In other words, the excitation mechanism may lead to an initial nonrandom distribution of molecular states (nonuniform phase space density) in the ground electronic state and then to branching ratios substantially different from those predicted by the RRKM theory. Bunker and Hase [11] named this type of behavior as apparently non-RRKM. Now, it is important to note that Lee's conclusions were inferred in the light of a mechanism with neither isomerization nor hydrogen scrambling (i.e., random exchange of hydrogen atoms). In fact they recognized that one source of disagreement might be a substantial hydrogen scrambling and/or isomerization in ethylene and its deuterated derivatives, but they disregarded it arguing that the experimental findings show no (complete) isomerization, that is, different branching ratios were observed for *cis*- and *trans*-HDCCDH. However, very recently, in a direct classical trajectory study we found that, at 193 and 157 nm of excitation, hydrogen scrambling on the electronic ground state is important [12]. Furthermore, we found a reasonable agreement between the calculated and the experimental H_2:HD:D_2 branching ratios. This agreement and the fact that the classical trajectories predicted that an initial microcanonical ensemble of excited ethylene is maintained during the decomposition (especially at 193 nm) led us to conclude that the photodissociation dynamics of ethylene (at the above energies) is occurring at, or near, the statistical limit if the excitation process leads to a statistical distribution of vibrational states on the ground electronic state (after internal conversion). As noticed in our previous work [12], we remark here that statistical dynamics in the ethylene dissociation does not mean that complete isotopic scrambling must occur on the time scale of reaction, as stated elsewhere [2], because hydrogen scrambling is a reactive event in itself rather than a vibrational movement.

Further insights into the dynamics behavior of the photodissociation of ethylene may be gained from the analysis of product energy distributions (PEDs). Accordingly, in this Letter we analyze the PEDs for the molecular hydrogen eliminations (reactions 1a and 1b) obtained by B3LYP/6-31G(d) direct trajectories initialized at the barriers with microcanonical (i.e., random) samplings at an energy corresponding to a photon excitation of 193 nm. Trajectory initialization at the barrier is frequently employed when one is interested in the calculation of PEDs in unimolecular reactions. This approach is supported by the fact that comparisons between classical and quantum dynamics show that classical dynamics gives accurate results for a direct process like a motion down a potential energy barrier [13]. The PEDs calculated in this study will be compared with the available experimental data. Since a microcanonical distribution at the barrier is consistent with RRKM dynamics, a good agreement between the trajectory and the experimental PEDs would provide additional support to Bersohn's conclusion that the dissociation takes place from a hot internally equilibrated ground state ethylene.

2. Methodology

In this Letter we employ a B3LYP/6-31G(d) direct trajectory method that takes the energy and derivatives of the potential energy surface (PES) directly from GAUSSIAN 98 [14]. Owing to the expense of the DFT direct dynamics, this investigation was limited to ensembles of fairly short time trajectories initiated at the exit-channel barrier for reactions 1a (ts2) and 1b (ts4) (see Fig. 1 in this Letter and Fig. 2 in [5]).

Table 1 collects some features of the stationary points of the B3LYP/6-31G(d) potential energy surface of our interest (those from the barrier to the products), in comparison with the high level results of Chang et al. [5]. In addition, the main

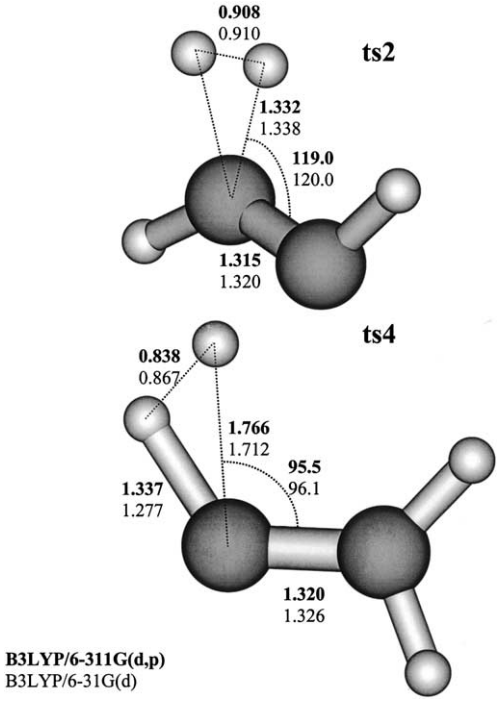

Fig. 1. Some geometrical parameters of the transition states ts2 and ts4 from which the trajectories are initiated. A comparison between the B3LYP/6-311G(d,p) (upper values in bold) and the present B3LYP/6-31G(d) (lower values) is also shown.

geometrical parameters of transition states ts2 and ts4 at the B3LYP/6-31G(d) and B3LYP/6-311G(d,p) [5] levels are compared in Fig. 1. As expected, the frequencies and geometries calculated in this work are very similar to those of Chang et al. [5], because in both cases they were computed by B3LYP calculations. The reverse barriers are also in good agreement with their CCSD(T) calculations. Therefore, the level of theory used to compute the ethylene exit channel PES is accurate enough for the present dynamics study.

The trajectories were initialized at transition states ts2 and ts4 with two barrier sampling methods. First, using a quasiclassical rigid rotor/normal mode procedure (here in after QRR/NM), which has been described in detail elsewhere [15,16]. Second, by a modification of the efficient microcanonical sampling (EMS) [17,18], referred to in a previous work as efficient microcanonical sampling in normal modes (EMSNM) [19], with which good results were obtained for the related 1,2-difluoroethylene systems [20]. In the EMSNM, the Cartesian coordinates of the system were selected by a Markov walk propagated along the $3N - 7$ normal mode coordinates, with the energy obtained from the DFT PES, thus allowing anharmonicity and coupling effects to be incorporated in the sampling. Contrary to the QRR/NM sampling, this is a classical method in which the effects of the zero point vibrational energy (ZPVE) are neglected. A modification of the EMS to include quantum ZPVE effects was carried out by Marks [21], but this method is only practical for very high energies in comparison with the ZPVE and therefore it was not employed here.

With the above algorithms we constructed microcanonical ensembles at the corresponding barriers (ts2 and ts4) for a total excitation energy of 193 nm and total angular momentum $J = 0$. Each ensemble comprises 300 trajectories, which were

Table 1
Some attributes of the B3LYP/6-31G(d) PES, in comparison with higher level theoretical results and experiment

	B3LYP/6-31G(d)	Higher level theoretical and experiment[a]
ts2 vibrational frequencies (cm^{-1})	1535*i*, 552, 762, 839, 1007, 1044, 1384, 1470, 1617, 2658, 3134, 3239	1650*i*, 540, 767, 788, 1033, 1052, 1404, 1446, 1633, 2585, 3151, 3272
ts4 vibrational frequencies (cm^{-1})	799*i*, 615, 683, 801, 901, 907, 1387, 1557, 1790, 2721, 3150, 3245	634*i*, 586, 608, 764, 860, 887, 1343, 1436, 1684, 3047, 3116, 3223
$E_{rev,2}$ (kcal mol^{-1})[b]	63.0	65.3
$E_{rev,4}$ (kcal mol^{-1})[b]	7.8	7.7
H_2 equilibrium bond length (Å)	0.743	0.744 (0.741)
H_2 vibrational frequency (cm^{-1})	4453	4416 (4401)

[a] From [5]: B3LYP/6-311G(d,p) results for frequencies and H_2 bond length and CCSD(T)/6-311+G(3df,3p) calculations at the B3LYP/6-311G(d,p) optimized geometries for energies. Experimental values (in parentheses) from [25].

[b] Reverse barriers. Energy difference between ts4 and: $CCH_2 + H_2$ or ts2 and $HCCH + H_2$.

integrated by using a combined fourth order Runge–Kutta and six-order Adams–Moulton predictor-corrector algorithm with a fixed step size of 0.1 fs. The cartesian forces and energies were obtained at the B3LYP/6-31G(d) level and, by using the optimized orbitals as the initial guess in subsequent force calculations, a substantial reduction in computer time was achieved.

The trajectories were propagated until the variation of the relative translational energy over five integration steps became smaller than 0.05 kcal mol^{-1}. This typically happens when the distance between the center-of-mass of the products is about 4 Å [1]. At this point the product relative translational energy, vibrational and rotational energies were calculated. Also the H_2 vibrational populations were computed by the Einstein–Brillouin–Keller (EBK) [22–24] quantization of the action integral.

All the trajectory calculations were accomplished by using a code that interfaces an extensively modified version of the classical trajectory program GENDYN [2] with the ab initio GAUSSIAN 98 [14] package.

3. Results and discussion

The trajectories were analyzed for product rotational (E_{rot,H_2} and $E_{rot,HCCH}$) and vibrational (E_{vib,H_2} and $E_{vib,HCCH}$) energies and $HCCH + H_2$ relative translational energy for each channel. Fig. 2 shows the translational energy distributions found here for channels 1a and 1b with the QRR/NM and EMSNM methods of initialization. Additionally, we show a comparison between the experimental translational energy distribution [1] and that computed here by using averaged results. Specifically, as a weighting factor, we used the 1a/1b branching ratio obtained by Chang et al. [5] from RRKM calculations (0.1575/0.5722) rather than the experimental ratio, because the latter may be uncertain as it was deduced from a mechanism with no scrambling. Plot c in Fig. 2 also displays the uncertainty in the trajectory distribution. The uncertainty in the occurrence number n_i of event i out of a sample of size n is given by

$$\Delta n_i = t n_i \left(\frac{n - n_i}{n_i n} \right)^{1/2}, \quad (1)$$

where t is the t student value for the desired confidence level of 95%. As seen in the figure, the DFT dynamics averaged results agree pretty well (within statistical errors) with the experimental curve of

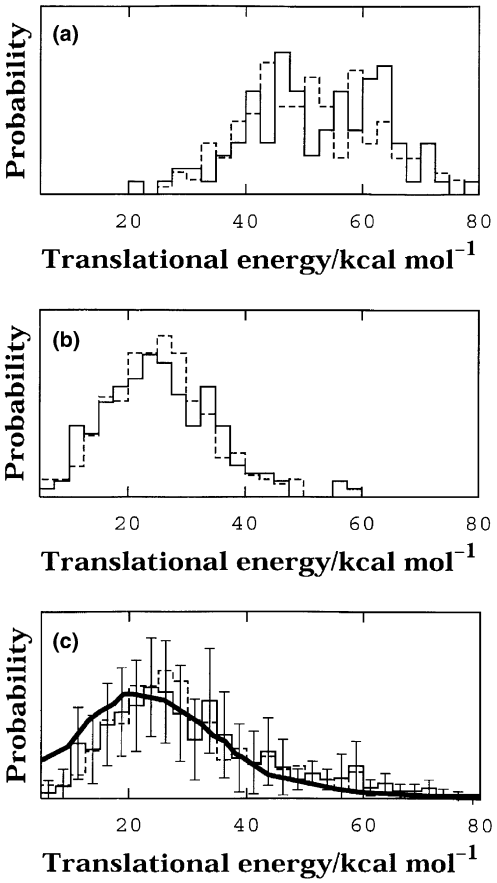

Fig. 2. Translational energy distributions obtained in the present study at 193 nm with the EMSNM (histograms with solid line) and QRR/NM (histograms with dashed line) excitation models for channels (a) 1a, (b) 1b and (c) a combination of both using the RRKM results of [5] In this last case the experimental [1] curve (solid thick line) is also depicted. In addition the uncertainties are evaluated from Eqs. (1a) and (1b) at a 95% confidence level.

[1] To assess the reliability of this approach, we followed some trajectories for a longer time, and found that the PEDs did not vary significantly.

[2] D.L. Thompson, GENDYN program.

Table 2
Average product energies (in kcal mol^{-1}) obtained in the 193 nm photodissociation of ethylene

	E_{trans}	E_{rot,H_2}	E_{vib,H_2}	$E_{rot,HCCH}$	$E_{vib,HCCH}$
Channel 1a					
QRR/NM	51.5	7.6	10.3	5.6	51.1
EMSNM	52.6	8.1	12.1	5.9	47.4
Channel 1b					
QRR/NM	25.5	7.8	12.3	3.5	77.0
EMSNM	25.5	7.3	10.8	5.2	77.3
Averaged results					
QRR/NM	31.1	7.8	11.9	4.0	71.3
EMSNM	31.3	7.5	11.1	5.4	70.8

Balko et al. [1]. In our previous study of the photodissociation of ethylene [12] we found that at 193 nm of excitation an initial microcanonical ensemble is maintained throughout the complete decomposition, in other words, the dynamics is intrinsically RRKM [11]. Therefore, the above results are consistent with the conclusion that the photodissociation takes place from a hot internally equilibrated ground state ethylene [8].

Average values for the translational, rotational and vibrational energies of the products are listed in Table 2. The main difference between the results of the 1a and 1b channels concerns the relative translational and HCCH vibrational energies. While the results of channel 1a give an average translational energy of 51.5 kcal mol^{-1}, those of channel 1b give half this value. This energy difference is almost channeled into the HCCH vibrational energy in channel 1b, and may be easily understood by a simple inspection of the related reverse barrier heights. The results for both QRR/NM and EMSNM methods of initialization are very similar, except for the rotational energy of the HCCH fragment in channel 1b for which EMSNM affords about 50% more rotational excitation of the fragment. This result may be related to the different nature of the samplings, that is, the EMSNM is anharmonic and takes into account the vibrational coupling. This may promote the vibrational excitation of the disappearing bending modes, which correlate with products rotation.

Fig. 3 compares the DFT trajectory results for the rotational state distributions of H_2 ($v = 0$) with the experimental data from [2] (plot c). In this

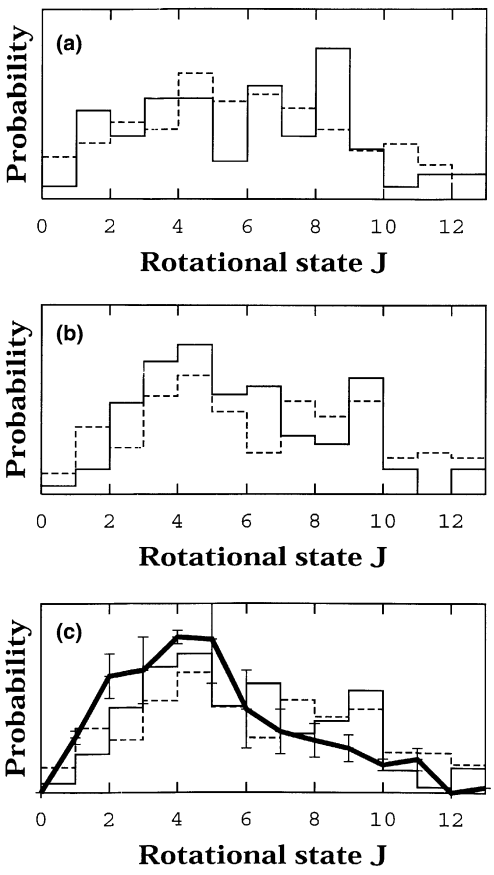

Fig. 3. Rotational state distributions obtained in the present study at 193 nm with the EMSNM (histograms with solid line) and QRR/NM (histograms with dashed line) excitation models for channels (a) 1a, (b) 1b and (c) a combination of both using the RRKM results of [5]. In this last case the experimental curve (solid thick line, [2]) is also depicted with the reported uncertainties.

Table 3
Vibrational populations of H_2 produced in the 193 nm photodissociation of ethylene

	Exp.[a]	QRR/NM	EMSNM
$v = 0$	85	81 ± 7	88 ± 8
$v = 1$	25	28 ± 6	22 ± 8
$v = 2$	7.4	9.0 ± 4	7.8 ± 6
$v = 3$	1.5	0.5 ± 1	1.1 ± 1

[a] Taken from [2].

case, the experimental uncertainties are also included. As above, the theoretical results in plot c are the averages of channels 1a and 1b, weighted by the RRKM branching ratio 1a/1b. For both theoretical and experimental distributions the peak is around 4–5 and for rotational states $J > 12$ the distribution vanishes. Note that in this case we have not shown the uncertainties in the theoretical distributions to make the graph clearer; however, the error bars are as large as the experimental ones. Thus, overall the agreement between experiment and theory is again quite satisfactory.

Finally, Table 3 displays the vibrational populations of H_2 at 193 nm obtained experimentally and the averaged DFT dynamics outcomes with the errors estimated at the 95% of confidence level. For $v = 0$ and $v = 1$ the experimental population is in between the theoretical results for both excitation models, and for $v = 2$ and $v = 3$ they are within the theoretical uncertainties.

In summary, the agreement between our dynamics results and experiment is good. Because the trajectories were microcanonically initiated at the barrier, the results suggest that the dynamics in the reactant phase space is ergodic.

4. Conclusions

In this work DFT direct trajectory simulations were carried out to study further the photodissociation of ethylene at 193 nm. The trajectories were initialized from the two exit barriers associated to molecular hydrogen formation. The average translational energy of the three-center channel 1b is half that of channel 1a, which presents a very large reverse barrier. The results obtained here under two different barrier sampling models agree quite well between each other, except for the HCCH rotational energies. This discrepancy may arise from the different nature of the Hamiltonian employed in the samplings.

When we employ the RRKM branching ratios for channels 1a and 1b as a weighting factor for averaging the dynamics results, the translational energies, H_2 rotational and vibrational states distributions agree quite well with experiment. These results together with those obtained in our previous study [12] show that there are no reasons to conclude that the dynamics is nonstatistical, which contrasts with the suggestions of Lee and coworkers. Our results are consistent with Bershon's statement that the dissociation takes place from a hot internally equilibrated ground state molecule (after internal conversion).

Acknowledgements

We are pleased to acknowledge financial support from Ministerio de Ciencia y Tecnología (BQU2000-0462). E.M.-N. and A.F.-R. also thank the above ministry of their Ramón y Cajal research contracts. A.P.-G. also acknowledges Ministerio de Ciencia y Tecnología for a F.P.U. grant.

References

[1] B.A. Balko, J. Zhang, Y.T. Lee, J. Chem. Phys. 97 (1992) 935.
[2] E.F. Cromwell, A. Stolow, M.J.J. Vrakking, Y.T. Lee, J. Chem. Phys. 97 (1992) 4029.
[3] A. Stolow, B.A. Balko, E.F. Cromwell, J. Zhang, Y.T. Lee, J. Photochem. Photobiol., A 62 (1992) 285.
[4] A.H.H. Chang, A.M. Mebel, X.-M. Yang, S.H. Lin, Y.T. Lee, Chem. Phys. Lett. 287 (1998) 301.
[5] A.H.H. Chang, A.M. Mebel, X.-M. Yang, S.H. Lin, Y.T. Lee, J. Chem. Phys. 109 (1998) 2748.
[6] J.J. Lin, D.W. Hwang, Y.T. Lee, X. Yang, J. Chem. Phys. 109 (1998) 2979.
[7] A.H.H. Chang, D.W. Hwang, X.-M. Yang, A.M. Mebel, S.H. Lin, Y.T. Lee, J. Chem. Phys. 110 (1999) 10810.
[8] S. Satyapal, G.W. Johnston, R. Bersohn, J. Chem. Phys. 93 (1990) 6398.
[9] M. Hayashi, A.M. Mebel, K.K. Liang, S.H. Lin, J. Chem. Phys. 108 (1998) 2044.

[10] E.M. Evleth, A. Sevin, J. Am. Chem. Soc. 103 (1981) 7414.
[11] D.L. Bunker, W.L. Hase, J. Chem. Phys. 59 (1973) 4621.
[12] A. Peña-Gallego, E. Martínez-Núñez, S.A. Vázquez, Chem. Phys. Lett. 353 (2002) 418.
[13] A. Untch, R. Schinke, R. Cotting, J.R. Huber, J. Chem. Phys. 99 (1993) 9553.
[14] M.J. Frisch et al., GAUSSIAN 98, Gaussian Inc., Pittsburgh, PA, 1998.
[15] C. Doubleday Jr., K. Bolton, G.H. Peslherbe, W.L. Hase, J. Am. Chem. Soc. 118 (1996) 9922.
[16] K. Bolton, W.L. Hase, G.H. Peslherbe, Modern Methods for Multidimensional Dynamics in Chemistry, World Scientific, Singapore, 1998.
[17] G. Nyman, S. Nordholm, H.W. Schranz, J. Chem. Phys. 93 (1990) 6767.
[18] H.W. Schranz, S. Nordholm, G. Nyman, J. Chem. Phys. 94 (1991) 1487.
[19] E. Martínez-Núñez, S.A. Vázquez, A.J.C. Varandas, Phys. Chem. Chem. Phys. 4 (2002) 279.
[20] J. González-Vázquez, E. Martínez-Núñez, A. Fernández-Ramos, S.A. Vázquez, J. Phys. Chem. A (in press).
[21] A.J. Marks, J. Chem. Phys. 108 (1998) 1438.
[22] A. Einstein, Verh. Dtsch. Phys. Ges. (Berlin) 19 (1917) 82.
[23] M.L. Brillouin, J. Phys. (Paris) 7 (1926) 353.
[24] J.B. Keller, Ann. Phys. (NY) 4 (1958) 180.
[25] Data from NIST Standard Reference Database 69 – July 2001 Release: *NIST Chemistry WebBook*.